
ARTICLE

Characterization of quasi-monoenergetic neutron source using 137, 200, 246 and 389 MeV ${}^7\text{Li}(p,n)$ reactions

Yosuke Iwamoto^{a*}, Masayuki Hagiwara^b, Hiroshi Iwase^b, Hiroshi Yashima^c, Daiki Satoh^a, Tetsuro Matsumoto^d, Akihiko Masuda^d, Christian Pioch^e, Vladimir Mares^e, Tatsushi Shima^f, Atsushi Tamii^f, Kichiji Hatanaka^f and Takashi Nakamura^g

^aJapan Atomic Energy Agency, 2-4 Shirakata, Tokai-mura, Naka-gun, Ibaraki-ken, 319-1195, Japan; ^bHigh Energy Accelerator Research Organization, 1-1 Oho, Tsukuba-shi, Ibaraki-ken, 305-0801, Japan; ^cResearch Reactor Institute, Kyoto University, 2-1010 Asashiro-nishi, Kumatori-cho, Sennan-gun, Osaka-hu, 590-0494, Japan; ^dNational Institute of Advanced Industrial Science and Technology, 1-1-1 Higashi, Tsukuba-shi, Ibaraki-ken, 305-8561, Japan; ^eGerman Research Center for Environmental Health, Institute of Radiation Protection, Ingolstadter Landstr. 1, 85764 Neuherberg, Germany; ^fResearch Center for Nuclear Physics, 10-1 Mihogaoka, Ibaraki-shi, Osaka-hu. 567-0047, Japan; ^gShimizu Corporation, 4-17, Etchujima 3-Chome, Koto-ku, Tokyo-to, 135-8530, Japan

The authors measured the neutron energy spectra of a quasi-monoenergetic ${}^7\text{Li}(p,n)$ neutron source with 137, 200, 246 and 389 MeV protons set at seven angles (0° , 5° , 10° , 15° , 20° , 25° and 30°), using a time-of-flight (TOF) method employing organic scintillators NE213 at the Research Center for Nuclear Physics (RCNP) of Osaka University. The energy spectra of the source neutrons were precisely deduced down to 2 MeV at 0° and 10 MeV at other angles. Neutron energy spectra below 100 MeV at all angles were comparable, but the shapes of the continuum above 150 MeV changed considerably with the angle. In order to consider the correction required to derive the response in the peak region from the measured total response for high-energy neutron monitors, the authors showed the subtractions of $\text{H}^*(10)$ obtained at larger angles from the 0° data in the continuum part. It was found that subtracting the dose equivalent at larger angles (21° for 389 MeV, 25° for 246 MeV and 26° for 200 MeV) from the 0° data almost eliminates the continuum component. This method has potential to eliminate problems associated with continuum correction for high-energy neutron monitors.

Keywords: quasi-monoenergetic neutron; lithium; neutron energy spectrum; continuum correction; RCNP

1. Introduction

Radiation fields behind accelerator shielding and flight altitudes are characterized by a large contribution of neutrons with energies above 20 MeV. When investigating neutron fields in such places, integrating detectors such as Bonner spheres, ionization chambers and dosimeters have been used with newly developed methods. Determining the reliability of detector response matrices requires calculations using Monte Carlo codes and calibration measurements. Quasi-monoenergetic neutron reference beams are of special importance for calibrating the detectors.

Facilities such as the iThemba [1] have quasi-monoenergetic neutron fields with energies up to 200 MeV using ${}^7\text{Li}(p,n_0){}^7\text{Be}$ (g.s. + 0.429 MeV, $Q = -1.64$ and -2.08 MeV). On the other hand, the Research Center for Nuclear Physics (RCNP) cyclotron facility has neutron fields in energy regions up to 400 MeV, and neutron energy spectra at 0° for 352 MeV protons have been measured [2]. These neutron energy spectra at 0°

have not only peak neutrons but also low-energy continua caused by breakup and spallation reactions. The fraction of the peak component in the neutron spectrum is around 50 %, but data correction for the contribution of continuum neutrons disturbs to derive the response in the peak region from the measured total response. Nolte et al. reported an interesting method to reduce the contribution experimentally at iThemba using the 100 MeV ${}^7\text{Li}(p,n)$ reaction [3]. They concluded that subtracting the data obtained at 16° from the 0° data provides a true monoenergetic spectrum because the spectrum of the continuum component is almost the same at 0° and at 16° . Although this method has the potential to eliminate problems associated with continuum correction, the neutron energy spectrum at larger angles for 100 - 400 MeV proton incident reactions has never been measured and the continuum correction has never been investigated.

This paper considers the measurement of neutron energy spectra at seven angles (0° , 5° , 10° , 15° , 20° , 25° and 30°) for the 140, 200, 246 and 389 MeV ${}^7\text{Li}(p,n)$ reactions at RCNP, and the characterization of peak and

*Corresponding author. Email: Iwamoto.Yosuke@jaea.go.jp

low-energy continua of neutron energy spectra in energy regions above 10 MeV.

2. Measurement

The experiments were performed in the 100 m tunnel of the RCNP ring cyclotron of Osaka University with 137, 200, 246 and 389 MeV protons, respectively; the beam current was 10–60 nA. A schematic of the experimental arrangement is shown in **Figure 1**. The experimental setup and data analysis were almost the same as that for our previous measurement [4].

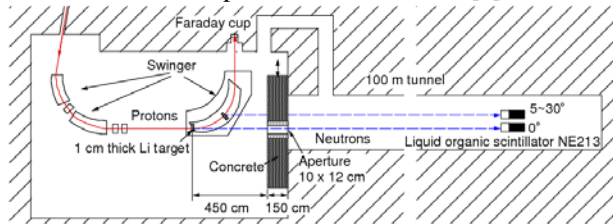


Figure 1. Illustration of experimental set up in the neutron experimental hall.

The proton beam extracted from the ring cyclotron was transported to the neutron experimental hall and hit a 1.0-cm-thick lithium target (${}^7\text{Li}$ 99.88 atom%) placed in the swinger, which was placed in a vacuum chamber. To measure the proton beam intensity, we used a swinger magnet to deviate the protons into a Faraday cup after they passed through the target. The uncertainty of the beam current measurement was estimated to be 1 % from the result of target-in and -out measurements. Neutrons produced at the target entered the 100 m tunnel through a 10 cm by 12 cm aperture in a 150-cm-thick movable iron collimator embedded in a concrete wall located 4.5 m from the target. At 20 m from the target, the radius of the neutron beam was about 22 cm. The clearing magnet in the movable collimator reduced the number of charged particles contaminating the neutron beam. The movable collimator and the swinger magnet allowed neutron emission to be measured for angles between 0° and 30° .

This facility is perfectly suited for a TOF study because the available flight path is about 100 m long. The neutron TOF measurements were performed at 0° , 5° , 10° , 15° , 20° and 25° for 137 and 200 MeV and 30° for 246 and 389 MeV using three different-sized NE213 organic liquid scintillators (25.4 by 25.4 cm, 12.7 by 12.7 cm, 5.08 by 5.08 cm, in diameter and length), each performing measurements at a different target–detector–surface distance. **Table 1** summarizes the detector settings, such as neutron energy ranges, detector sizes and flight path length.

Table 1. Summary of detector setting to neutron energy.

Neutron energy	3–10 MeV	10–100 MeV	100–MeV
Diameter and thickness	5.08 cm	12.7 cm	25.4 cm
Flight path	7 m	17–20 m	60–95 m

For the 7 m measurements, a 5-mm-thick plastic scintillator (NE102A) placed in front of the detector tagged events induced by charged particles. To obtain good energy resolution in the high-energy region, we performed long-path measurements using the NE213 with 25.4 cm length. The time width of proton beam bunch was about 1 ns. To avoid contamination with lower-energy neutrons, the time intervals between the successive proton-beam pulses were enlarged to 500 ns using a beam chopper. These time intervals correspond to frame-overlap neutron energies of about 90 MeV at 95 m, about 10 MeV at 20 m, and about 1 MeV at 7 m.

Data were recorded using a conventional computer-automated measurement and control system in the event-by-event mode. For each event, we recorded the magnitude of the total and slow components of the pulse from the neutron-detector photomultiplier tube, as measured by a charge-sensitive analog-to-digital converter (ADC), to discriminate neutron events from gamma-ray events [4]. We used the TOF method to determine the neutron energy. Hence, for each event, we recorded the time difference between the chopper signal from the cyclotron and the neutron detector, as measured by a time-to-digital converter (TDC).

The neutron detection efficiency of NE213 was calculated using the SCINFUL-QMD code [5]. To investigate the effect of the neutrons scattered into the collimator, on the wall, and the floor for TOF measurements, TOF distributions for neutron events in the detectors were calculated using PHITS [6] and with the real geometry of the RCNP TOF tunnel [4]. The results show that the number of background neutrons above 3 MeV is less than 1% of the number of foreground neutrons. Therefore, the contribution of background neutrons to TOF measurements above 3 MeV was negligible.

Uncertainties in TOF measurements were due to statistical and systematic errors. The statistical uncertainties were below 3 %. The systematic error arose mainly from neutron detection efficiency which is estimated to be 15 % [7]. The energy resolution was 0.5, 0.8, and 2.9 MeV for 137, 200, and 389 MeV neutrons at 95.5 m, respectively. For 246 MeV neutrons at 60 m, it was 2.3 MeV.

3. Results

3.1. Neutron energy spectra

Figure 2 shows a comparison of measured neutron energy spectra at 0° for 137, 200, 246 and 389 MeV using 1 cm thick lithium target with the data by Nakao et al. [8] for 90 MeV and Taniguchi et al. [2] for 352 MeV. The cross-sections of ${}^7\text{Li}(p,n_0,1){}^7\text{Be}$ in the proton energy region from 80 to 400 MeV are about 36 mb in the LAB system [4]. The small peaks 10 and 30 MeV lower than the peak arose from the transition to the high-energy excited state of ${}^7\text{Be}$. The quasifree (QF) region represents a broad peak in the nuclear continuum that may be viewed as an elastic collision of the incident

particle with a single target near the nuclear surface [4]. The continuum with $20 \text{ MeV} < E_n < 100 \text{ MeV}$ was mainly from the three-body break up process ${}^7\text{Li}(p,n{}^3\text{He})\alpha$, while the low-energy part with $E_n < 20 \text{ MeV}$ was from evaporation processes [4]. Most of the continuum of data comes directly from $\text{Li}(p,xn)$ reaction because there are less than 1 % room-scattered neutrons with $E_n > 3 \text{ MeV}$ to the reaction neutrons [4].

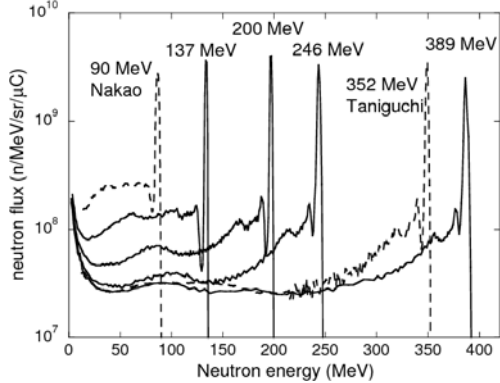


Figure 2. Comparison of measured neutron energy spectra for the 137, 200, 246 and 389 MeV $\text{Li}(p,xn)$ reaction at 0° with the data by Nakao et al. [7] and Taniguchi et al. [2].

The neutron intensity of the high-energy peak at 0° was about $1 \times 10^{10} \text{ (n/sr/}\mu\text{C)}$ and was not dependent on incident proton energy. The contribution of peak intensity to the total intensity varied between 0.4 and 0.5 in the incident proton energy range from 90 to 389 MeV. Therefore, the corrections required to derive the response can be considerable.

Figure 3 shows angular distributions of neutron energy spectra for 137, 200, 246 and 389 MeV $\text{Li}(p,xn)$ reactions at angles of $0^\circ, 5^\circ, 10^\circ, 15^\circ, 20^\circ$ and 25° for 137 and 200 MeV and 30° for 246 and 389 MeV. All neutron energy spectra in the energy region below 50 MeV were comparable, but the shape of the continuum in the QF region above 100 MeV changed considerably with the angle and incident proton energy.

3.2. Neutron dose equivalent

To investigate the angular distribution of response of monitors in the mono-energetic neutron field, the authors estimated the ambient dose equivalent $H^*(10)$ at

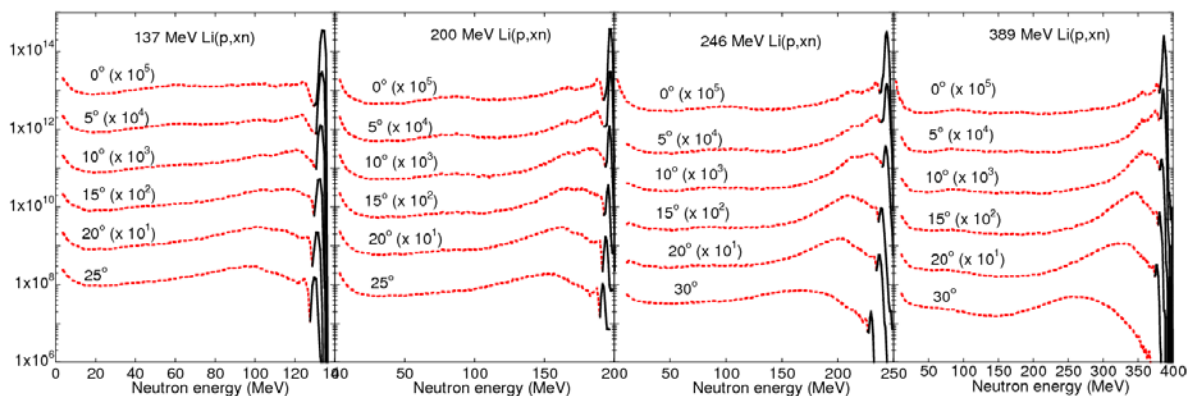


Figure 3. Experimental results of neutron energy spectra at $0^\circ, 5^\circ, 10^\circ, 15^\circ, 20^\circ, 25^\circ$ and 30° for 137, 200, 246 and 389 MeV. Solid line indicates the peak region of spectrum and dashed line shows the continuum part.

20 m from a target using the ambient dose equivalent coefficient, $C(E_n)$, taken from Ref. [9] and measured neutron energy spectra, $\phi(E_n)$, by the following equation:

$$H^*(10) = \int C(E_n)\phi(E_n)dE_n \quad (1)$$

The ambient dose equivalent coefficient was selected because the shape of the dose conversion factor for the high-energy neutron monitors such as WENDI-2 and DARWIN is almost same with that of the ambient dose equivalent coefficient [4]. Figure 4 shows angular distribution of $H^*(10)$ at 20 m from a target. From this figure, one clearly sees that it is almost steady at angles below 25° for 137 MeV and below 15° for 200 MeV, while it gradually decreases with angles for 246 and 389 MeV. It is for reason that continuum component with neutron energy range from 10 MeV to maximum energy except for high-energy peak strongly contributes to total $H^*(10)$ while peak component decreases with angles.

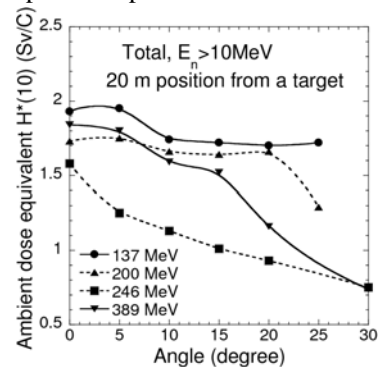


Figure 4. Angular distribution of $H^*(10)$ at 20 m from a target. The lines are only meant as a guide.

3.3. Correction of continuum part for monitor response

To reduce the contribution from the continuum, the authors considered the corrections required to derive the response using neutron spectra at larger angles. Figure 5 shows subtractions of $H^*(10)$ obtained at larger angles from the 0° data in the continuum part with $E_n > 10 \text{ MeV}$. This shows that most efficient angle to eliminate the contribution of the continuum part to the total $H^*(10)$ is 21° for 389 MeV proton, 25° for 246 MeV proton and 26° for 200 MeV proton, respectively. On the other hand, the subtraction method is not applicable to 137 MeV protons because neutron intensity in

continuum part at larger angles is higher than that at 0° . Note that we did not consider correction of continuum part below 10 MeV because neutron energy spectra at larger angles for 246 and 389 MeV were not measured due to the limited beam operation.

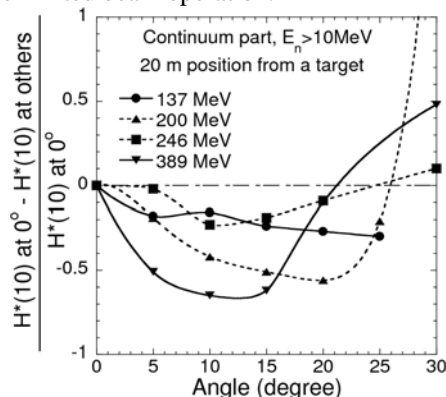


Figure 5. Difference ambient dose equivalent obtained at larger angles from the 0° data in the continuum part with $E_n > 10$ MeV. The extrapolation curve is plotted for 200 MeV.

4. Conclusion

The authors measured neutron energy spectra using ${}^7\text{Li}(p,n)$ reaction with 137, 200, 246 and 389 MeV protons at seven angles (0° , 5° , 10° , 15° , 20° , 25° and 30°). Peak neutron intensities at 0° were about 1×10^{10} (n/sr/MeV/ μC), and the peak neutron angular distribution agreed well with calculated results using the Taddeucci formula. Neutron energy spectra below 100 MeV at all angles were comparable, while the shape of the continuum above 150 MeV changed considerably with the angle. To consider the correction required to derive a response for high-energy neutron monitors, the authors proposed that subtracting the ambient dose equivalent obtained at larger angles (21° for 389 MeV, 25° for 246 MeV and 26° for 200 MeV) from the 0° data almost eliminates the continuum component above 10 MeV. The proposed method makes it possible to reduce uncertainty in the response in calibrations for high-energy neutron monitors.

References

- [1] W.R. McMurray, D.G. Aschman, K. Bharuth-Ram and R.W. Fearick, The faure cyclotron neutron source and a particle spectrometer for neutron induced emission of charged particles at energies between 60 and 200 MeV, *Nucl. Instr. and Meth. A* 329 (1993), pp. 217-222.
- [2] S. Taniguchi, N. Nakao, T. Nakamura, H. Yashima, Y. Iwamoto, D. Satoh, Y. Nakane, H. Nakashima, T. Itoga, A. Tamii and K. Hatanaka, Development of a quasi-monoenergetic neutron field using the ${}^7\text{Li}(p,n){}^7\text{Be}$ reaction in the energy range from 250 to 390 MeV at RCNP, *Rad. Prot. Dosim.* 126 (1-4) (2007), pp. 23-27.
- [3] R. Nolte, M.S. Allie, P.J. Binns, F. Brooks, A. Buffler, V. Dangendorf, J.P. Meulders, F. Roos, H. Schuhmacher and B. Wiegel, High-energy neutron reference fields for the calibration of detectors used in neutron spectrometry, *Nucl. Instr. and Meth. A* 476 (2002), pp. 369-373.
- [4] Y. Iwamoto, M. Hagiwara, D. Satoh et al., Quasi-monoenergetic neutron energy spectra for 246 and 389 MeV ${}^7\text{Li}(p,n)$ reactions at angles from 0° to 30° , *Nucl. Instr. and Meth. A* 629 (2011), pp. 43-49.
- [5] D. Satoh, T. Sato, N. Shigyo, K. Ishibashi, *SCINFUL-QMD: Monte Carlo based Computer Code to Calculate Response Function and Detection Efficiency of a Liquid Organic Scintillator for Neutron Energies up to 3 GeV*, JAEA-Data/Code, 2006-023, Japan Atomic Energy Agency, (2006).
- [6] K. Niita, N. Matsuda, Y. Iwamoto, H. Iwase, T. Sato, H. Nakashima, Y. Sakamoto and L. Sihver, *PHITS: Particle and Heavy Ion Transport Code System, Version 2.23*, JAEA-Data/Code, 2010-022, Japan Atomic Energy Agency, (2010).
- [7] Y. Iwamoto, M. Hagiwara, T. Matsumoto, A. Masuda, H. Iwase, H. Yashima, T. Shima, A. Tamii and T. Nakamura, Measurements and Monte Carlo calculations of forward-angle secondary neutron production cross sections for 137 and 200 MeV proton-induced reactions in carbon, *Nucl. Instr. and Meth. A* 690 (2012), pp. 10-16.
- [8] N. Nakao, Y. Uwamino, T. Nakamura, T. Shibata, N. Nakanishi, M. Takada, E. Kim and T. Kurosawa, Development of a quasi-monoenergetic neutron field using ${}^7\text{Li}(p,n){}^7\text{Be}$ reaction in the 70-210 MeV energy range at RIKEN, *Nucl. Instr. and Meth. A* 420 (1999), pp. 218-231.
- [9] T. Sato, A. Endo, M. Zankl, N. Petoussi-Henss, H. Yasuda and K. Niita, Fluence-to-dose conversion coefficients for aircrew dosimetry based on the new ICRP Recommendations, *Progress in Nuclear Science and Technology* 1 (2011), pp. 134-137.